

ENCIT-2018-0751

DESIGN AND ANALYSIS OF A GENERIC SCRAMJET AIR INLET

Paulo Gilberto de Paula Toro

Ramon Carneiro

Jonatha Wallace da Silva Araújo

George Santos Marinho

Universidade Federal do Rio Grande do Norte/UFRN - Centro de Tecnologia. Av. Senador Salgado Filho, 3000 - Campus Universitário, Lagoa Nova CEP 59.078-970 - Natal/RN - Brasil

toro@ct.ufrn.br, marcosabinop@gmail.com, jonatha_wallace@hotmail.com, gmarinho@ct.ufrn.br

Gilvan Luiz Borba

Universidade Federal do Rio Grande do Norte/UFRN - Centro de Ciências Exatas e da Terra. Av. Senador Salgado Filho, 3000 - Campus Universitário, Lagoa Nova, CEP 59.078-970 - Natal, RN - Brasil

gilvan@geofisica.ufrn.br

João Felipe de Araújo Martos

European Space Research and Technology Centre (ESTEC)-ESA, Keplerlaan 1, 2001 AZ Noordwijk, The Netherlands

Joao.Martos@esa.int

Israel da Silveira Rêgo

Instituto de Estudos Avançados/IEAv - Trevo Coronel Aviador José Alberto Albano do Amarante, nº1 Putim CEP. 12.228-001 São José dos Campos, SP - Brasil

israel.rego@ieav.ct.br

Abstract. *A generic hypersonic airbreathing propulsion based on supersonic combustion ramjet (scramjet) technology has been designed, at the Universidade Federal do Rio Grande do Norte (UFRN), using analytical theoretical analysis (engineering approach). A full-scale generic scramjet model configuration is based on the technological demonstrator scramjet 14-X S, in development at the Instituto de Estudos Avançados (IEAv). A two-dimensional hydrogen powered generic scramjet inlet has been designed to demonstrate, in atmospheric flight, a supersonic combustion, of atmospheric air (in supersonic speed) with hydrogen, on an acceleration mission to 2050 m/s (Mach number 6.8) at 30 km geometric altitude. In this preliminary design, one-dimensional compressible flow (shock wave) theory, which may readily describe many features of compression region of the airbreathing engine, is used to estimate the shock wave angles, thermodynamic properties and the velocities (Mach numbers) of the hypersonic atmospheric air flow, at the generic scramjet inlet. The scramjet engine is divided into several components based on key design parameters to assess the engine performance as a function of these parameters. One of the most important design aspects is the temperature at the entrance of the combustion chamber because the compression must provide enough high temperature, higher than ignition temperature of the hydrogen, for supersonic combustion with the supersonic atmospheric air, at the combustion chamber. The turning (deflection) angles of the compression section ramps are optimized by using the same total pressure (recovery) ratios across each incident oblique shockwave. Additionally, calculations are done in order to check if the momentum and the energy are conserved across each oblique shockwave.*

Keywords: *scramjet, supersonic combustion ramjet, hypersonic airbreathing propulsion*

1. INTRODUCTION

The aerospace technological products have been grown, that one cannot conceive of putting payloads (satellites) into Earth's orbit or beyond (to deep space) using technologies in operation (rockets carrying solid or liquid fuel). The knowledge required to keep the current launching vehicles is already so high that if the countries do not provide a technological support for their own aerospace industries, these countries will depend on the supplier countries and will not have independent capacity sustained. Aerospace vehicle limitations for launching payloads into Earth's orbit or beyond require a continuous reduction in size, weight and power consumption of launching vehicles. Some solutions to these challenges require paradigm shifts, new production methods, and new technologies of strategic nature. The requirements of platforms launching satellites, of high performance and reliability, as well as the strict limitations of fuel (reduction of size, weight and power consumption) for launching payloads into orbit or beyond provide the development of hypersonic aircraft using hypersonic airbreathing propulsion based on supersonic combustion ramjet (scramjet) technology.

Nowadays, scramjet technology is a topic that has been attracted the attention of several scientific communities (USA, Australia, Germany, France, Japan, India, China, Russia), and they are investing, in this kind of propulsion system, due to interest to facilitate access to space and to reach hypersonic speed.

The recent intensification of international efforts to develop on scramjet technology, signals that this is the way of effective access to space in a not too distant future. Therefore, scramjet technology will be essential in the near future for the aerospace industry and will be allowing the man to build hypersonic planes, to reach other continents in hours and achieve low orbits around Earth.

In 2007, Brazilian researchers, from Laboratório de Aerodinâmica e Hipersônica Prof. Henry T. Nagamatsu, at Instituto de Estudos Avançados (IEAv), proposed to design, to develop, to manufacture and to demonstrate, in free flight, a technological demonstrator using: i) waverider technology to provide lift to the aerospace vehicle, and ii) scramjet technology to provide hypersonic airbreathing propulsion system based on supersonic combustion (Rolim et al., 2009).

The fully airframe-integrated scramjet 14-X waverider (Fig. 1) and the scramjet 14-X S (Fig. 2) are being designed to demonstrate supersonic combustion during atmospheric flight in about 30 km of altitude, in hypersonic speeds corresponding to the numbers of Mach 10 (approximately 3000 m/s) and 7 (approximately 2100 m/s), respectively.



Figure 1. Demonstrator scramjet 14-X waverider.

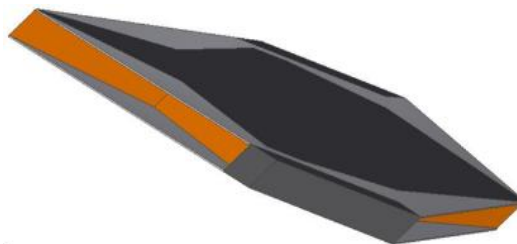


Figure 2. Demonstrator scramjet 14-X S.

Hypersonic airbreathing propulsion, that uses supersonic combustion ramjet (scramjet) technology, Figs. 1 and 2, offers substantial advantages to improve performance of aerospace vehicle that flies at hypersonic speeds through the Earth's atmosphere, by reducing onboard fuel. As a matter of fact, at hypersonic speeds (Fig. 3), a typical value for the specific impulse of a H_2-O_2 rocket engine (from the launch to Earth's orbit, Mach number 26) is about 400s, while the specific impulse of a H_2 fueled scramjet is 3000s to 400s, considering Mach numbers from 6 to 26, only up to 60 km altitude). In fact, the use of atmospheric air as oxidizer allows air breathing propulsion vehicles to substantially increase payload weight.

Basically, scramjet is a fully integrated airbreathing aeronautical engine, with no moving parts, that uses the oblique/conical shock waves generated during the hypersonic flight, to provide compression and deceleration of freestream atmospheric air at the inlet of the scramjet, which are pushed to combustion chamber (Fig. 4). Fuel, at least sonic speed, may be injected into the supersonic airflow just downstream of the inlet or at the beginning of the combustion chamber (combustor). Right after, both oxygen (from the atmospheric air) and on-board hydrogen fuel are mixed. The combination of the high energies of the fuel and of the oncoming supersonic airflow starts the combustion at supersonic speed. Finally, the divergent exhaust nozzle at the afterbody vehicle accelerates the exhaust gases, providing thrust.

In consequence of the nature of the scramjet engines, scramjets are unable to produce thrust while stationary. Solid-rocket engines may be used to accelerate the scramjet to a speed such that the shock waves produced by the air intake are able to compress the atmospheric air achieving the operational conditions (Hass et al., 2005). Such approach may provide an affordable path for maturing Brazilian hypersonic airbreathing components and subsystems in flight. The Brazilian hypersonic accelerator vehicle which is composed by two-stage (S31 and S30) solid rocket engines, unguided, rail launched, is able to accelerate the 14-X S to the predetermined flight test conditions of the scramjet operation (30

km altitude at Mach number 7) from one of the Brazilian Launch Centers (Centro de Lançamento de Alcântara, CLA, or Centro de Lançamento da Barreira do Inferno, CLBI).

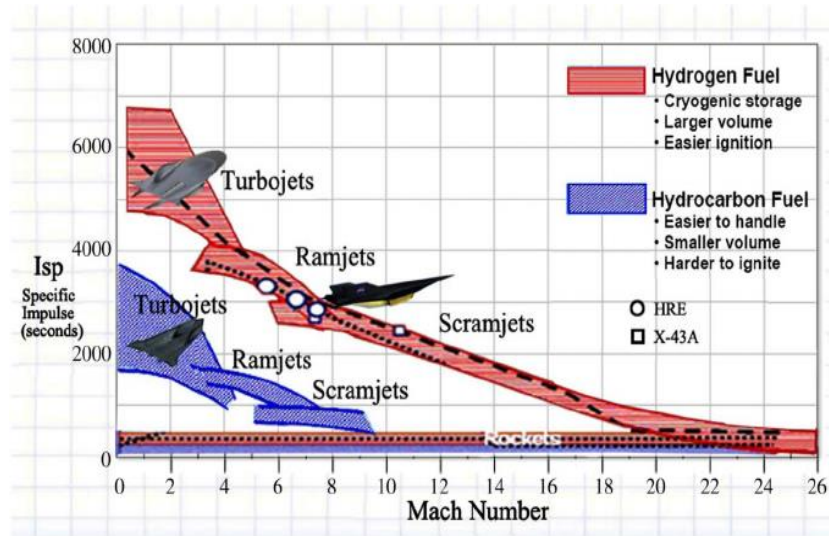


Figure 3. Specific impulse as function of the Mach number (Moses et al., 2004).

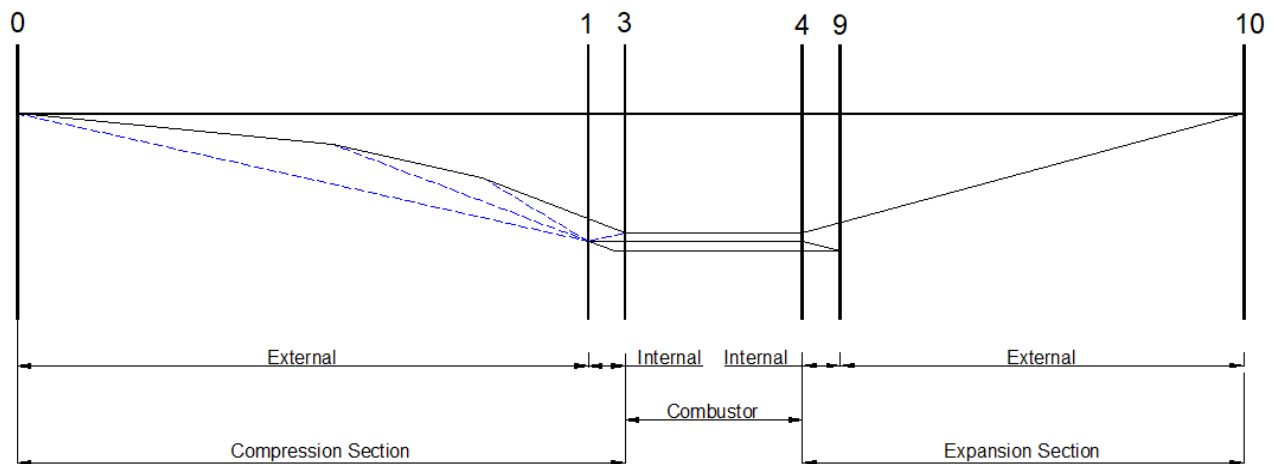


Figure 4. Airframe-integrated scramjet engine stations and reference terminology (adapted from Heiser and Pratt, 1994).

In order to contribute in training human resources and in execution of Research, Development and Innovation in strategic aerospace technologies, such as the Hypersonic Airbreathing Propulsion based on supersonic combustion, the concentration area of Aerothermodynamics and Hypersonics is being implemented at the Graduate Program in Mechanical Engineering, by Universidade Federal do Rio Grande do Norte (UFRN).

2. METHODOLOGY

2.1 Scramjet characteristics

First, it is necessary to establish a nomenclature to be used in the scramjet design. Heiser and Pratt (1994) present the terminology of the scramjet, which may be divided in three main components (Fig. 4): external and internal compression section (inlet), combustion chamber (combustor), and internal and external expansion section (outlet).

Stations 0 and 1 are the leading edges of the scramjet and of the cowl, respectively. Stations 3 and 4 are the entrance and exit of the combustion chamber. Stations 9 and 10 are the trailing edges of the cowl and the scramjet, respectively.

The external compression section is governed by incident shock wave, while the internal is governed by reflected shock wave. The internal and external expansion section is governed by expansion wave, Prandtl-Meyer Theory, and area ratio. The constant area section of the combustion chamber is called as isolator and is used to uniformize the flow from the compression section. Fuel is injected right after the isolator used to expand the gases from burning the fuel and

the oxygen. In general, one-dimensional flow with heat addition, Rayleigh flow, is used to simulate the burning the fuel and the oxygen.

An important feature of the scramjet is a highly integrated system, where engine and vehicle are indistinguishable. This tight integration is caused by the fact that the front section of the vehicle contributes to the compression of atmospheric air, while the rear contributes to the generation of thrust. The net thrust produced by the scramjet is the difference between the thrust (force that propels the vehicle) generated by the expansion of exhaust gases from the rear of the engine and the total drag (force that resists the movement of the vehicle). These forces may produce thrust to the flight of the vehicle or not depending on the balance of these forces in engine design in question.

Therefore, the operation of the scramjet engine obeys the (closed) Brayton thermodynamic cycle. Note the correspondence of Brayton cycle points (Fig. 5) with the reference stations of scramjet (Fig. 4). Observe that the heat addition should be evaluated as constant pressure section, because it avoids the possibility of boundary-layer separation and the necessity to design the structure to withstand the pressure peak. In order to obtain constant pressure section after fuel injection the area in this section should be divergent, but in the present paper this section will be constant (Fig. 4). Also, the static pressure at the exit, station 10, of the scramjet expansion section (trailing edge) should be very close of the freestream static pressure, station 0 (Fig. 5).

Finally, note that the incident shock waves (Fig. 6), from the external compression section, should incident on the leading edge of the cowl (shock on-lip) and the reflected shock wave, of the internal compression section, should incident on the entrance of the combustion chamber (shock on-corner). Therefore, the air capture area should be maximum and the length of the scramjet compression section should be minimum.

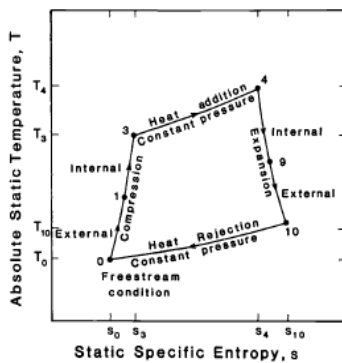


Figure 5. Brayton cycle temperature-entropy diagram (Heiser and Pratt, 1994).

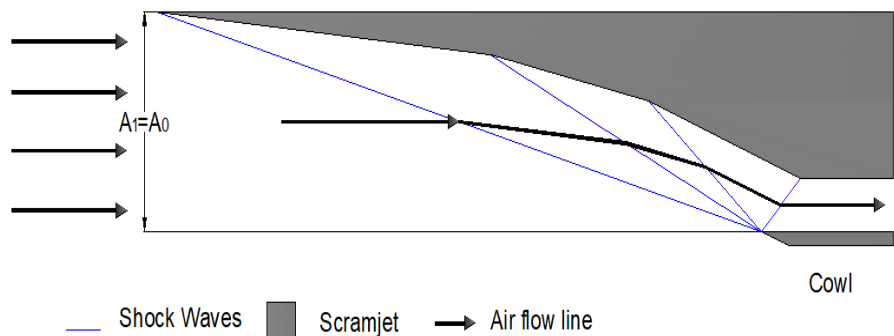


Figure 6. Schematic incident shock waves and reflected shock wave at the scramjet inlet.

2.2 Governing conservation laws

In the analytical theoretical analysis, the subscripts *in* and *out* are used to identify the upstream (inlet) and the downstream (outlet) conditions, respectively, of each station (Fig. 7) of the generic scramjet inlet baseline.

Considering no boundary-layer effects (non-viscous flow) and for calorically perfect gas ($p = \rho RT$, $\gamma = \text{constant}$) the mass, momentum and energy conservation laws (Anderson, 1990) in two-dimensional steady state, non-viscous, no heat conduction compressible flow, applied to plane oblique shock wave (Fig. 7), are given by:

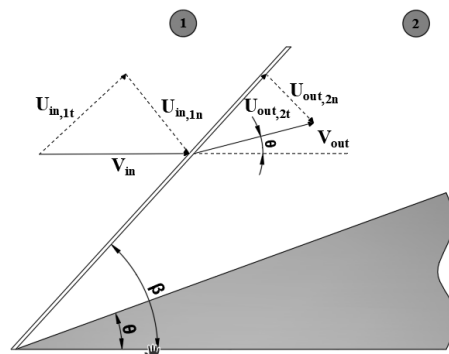


Figure 7: Leading edge incident plane oblique shock wave geometry.

$$\rho_{in} u_{in_n} = \rho_{out} u_{out_n} \quad (1)$$

$$p_{in} + \rho_{in} u_{in_n}^2 = p_{out} + \rho_{out} u_{out_n}^2 \quad (2)$$

$$u_{in_t} = u_{out_t} \quad (3)$$

$$h_{in} + \frac{u_{in_n}^2}{2} = h_{out} + \frac{u_{out_n}^2}{2} \quad (4)$$

where: ρ , p , u_{in_n} , u_{out_n} , u_{in_t} , u_{out_t} and h are density, pressure, normal and tangential velocities across the plane oblique shock wave and enthalpy of the gas, respectively.

2.3 Oblique shock wave relationships

Considering no boundary-layer effects (non-viscous flow) and for calorically perfect gas ($p = \rho RT$, $\gamma = \text{constant}$) the shock wave angle β (Fig. 7) is a function of the incoming local supersonic/hypersonic flow Mach number M_{in} , the gas from the atmosphere γ (air in the Earth's planet, $\gamma = 1.4$) and the deflection angle θ_s , and it may be obtained iteratively with the relationship given by (Anderson, 1990):

$$\text{tg} \theta_s = 2(\cotg \beta) \left[\frac{(M_{in} \text{sen} \beta)^2 - 1}{M_{in}^2 (\gamma + \cos 2\beta) + 2} \right] \quad (5)$$

Additionally, the oblique shock relationships can be easily obtained as closed form of the thermodynamic property (static pressure, static density, static temperature, ...) ratios and the Mach number across the oblique shock given by:

$$\frac{p_{out}}{p_{in}} = 1 + \frac{2\gamma}{(\gamma + 1)} \left[(M_{in} \text{sen} \beta)^2 - 1 \right] \quad (6)$$

$$\frac{\rho_{out}}{\rho_{in}} = \frac{(\gamma + 1)(M_{in} \text{sen} \beta)^2}{\left[(\gamma - 1)(M_{in} \text{sen} \beta)^2 + 2 \right]} \quad (7)$$

$$\frac{T_{out}}{T_{in}} = \frac{p_{out}}{p_{in}} \frac{\rho_{in}}{\rho_{out}} = \left\{ 1 + \frac{2\gamma}{(\gamma + 1)} \left[(M_{in} \text{sen} \beta)^2 - 1 \right] \right\} \frac{\left[(\gamma - 1)(M_{in} \text{sen} \beta)^2 + 2 \right]}{(\gamma + 1)(M_{in} \text{sen} \beta)^2} \quad (8)$$

$$M_{out} = \frac{\sqrt{\frac{(M_{in} \text{sen} \beta)^2 + \frac{2}{(\gamma - 1)}}{\frac{2\gamma}{(\gamma - 1)} (M_{in} \text{sen} \beta)^2 - 1}}}{\text{sen}(\beta - \theta_s)} \quad (9)$$

Note, the flow across the plane oblique shock wave promote an increase of pressure, density, temperature, and a decrease of Mach number, however the flow remains supersonic/hypersonic and parallel to the flat surface of the external compression section (Fig. 7) of the hypersonic vehicle with airframe-integrated scramjet engine lower surface.

Also, the leading-edge incident plane oblique shock wave theory may be used for incident oblique planar (Fig. 8) shock wave (compression ramp angle) and the reflected shock wave (Fig. 9).

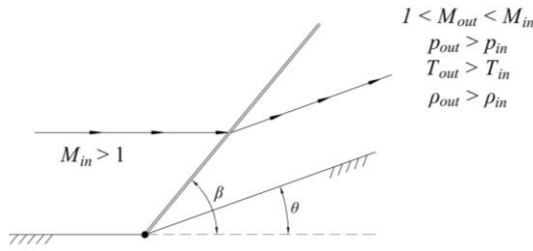


Figure 8. Leading edge incident plane oblique shock wave geometry (Anderson, 1990).

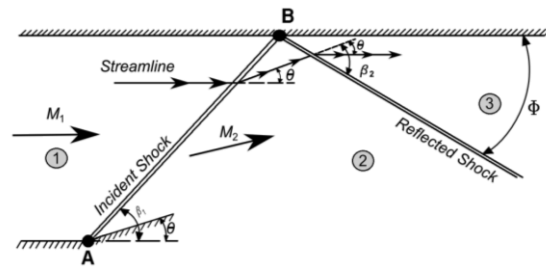


Figure 9. Reflected oblique shockwave geometry (Anderson, 1990).

2.4 Scramjet inlet design by total pressure recovery

Ran and Mavris (2005) defined an optimization criterion used to determine the ramp angles of the oblique shock waves for a maximum pressure recovery of the supersonic section. The optimization criterion was, first, proposed by Oswatitsch (1944) and may be applied for a system of $n-1$ oblique shocks and one normal shock in two dimensions (Fig. 10). The maximum shock pressure recovery is obtained when the shock waves are of equal strength, i.e., the Mach numbers perpendicular to the individual shock waves are equal, which the relationship is given by:

$$M_1 \sin \beta_1 = M_2 \sin \beta_2 = \dots = M_{n-1} \sin \beta_{n-1} \quad (10)$$

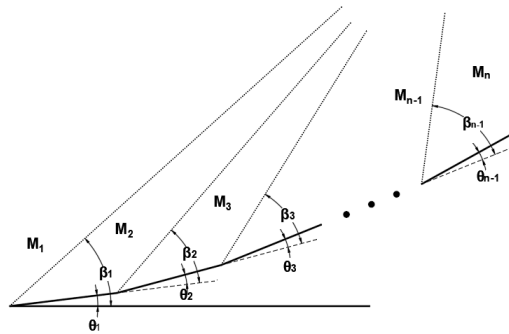


Figure 10. The optimization criterion to maximize total pressure recovery (Ran and Mavris, 2005).

The modified optimization criterion to maximize total pressure recovery, developed by Ran and Mavris (2005), was applied for hypersonic scramjet inlet (Martos, 2017), which the freestream hypersonic airflow is decelerated to the supersonic speed, at the combustion chamber, through a suitable shock system (including only oblique shock waves).

The total pressure recovery is presented by Heiser and Pratt (1994) as a parameter π , given by:

$$\pi = \frac{p_{te}}{p_{ti}} = \frac{p_e}{p_i} \left[\frac{\left(1 + \frac{\gamma-1}{2} M_e^2 \right)}{\left(1 + \frac{\gamma-1}{2} M_i^2 \right)} \right]^{\frac{\gamma}{\gamma-1}} \quad (11)$$

2.5 Maximum shockwave angles criterion

Also, in this scientific work is applied the criterion of maximum shockwave angles. According to Heiser and Pratt (1994) for flight about Mach number 7 the appropriate deflection angle, to minimize the boundary layer detachment and assure re-attachment of the boundary-layer, is close to 5° for laminar flow and 12° for turbulent flow (Fig. 11). Also, the difference between the initial shockwave and deflection angles should be about 8° for two oblique shockwaves and about 6° for more than four oblique shockwaves (Fig. 12).

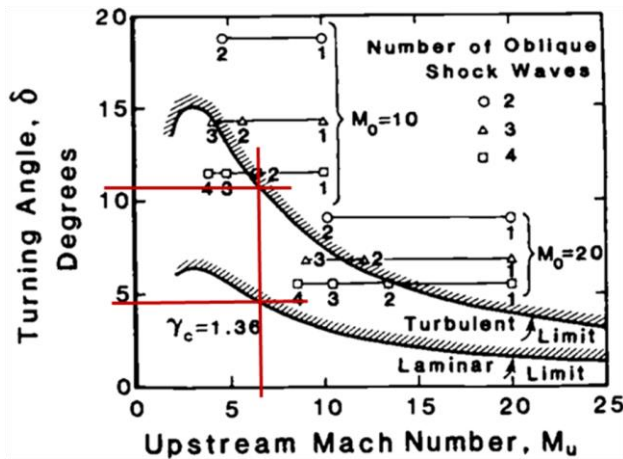


Figure 11. Maximum allowable turning angle without boundary-layer separation (Heiser and Pratt, 1994).

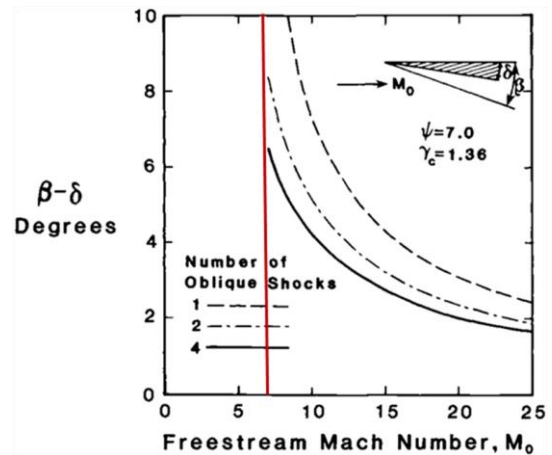


Figure 12. The initial oblique shockwave and the deflection angle difference (Heiser and Pratt, 1994).

3. RESULTS AND COMMENTARIES

First is necessary to define the thermodynamic atmospheric air properties, which the generic scramjet will perform atmospheric flight, at 30 km geometric altitude (Tab. 1) and speed corresponding to Mach number 6.8 (Tab. 2).

Observe that the Knudsen number is very low, $4.45113 \cdot 10^{-6}$ ($Kn \leq 0.01$), so the mass, momentum and energy conservation laws, based on the Navier-stokes, should be applied for continuum flow (dense Earth's atmospheric air). Also, the flow over the scramjet is more like a turbulent flow with Reynolds number of $2.56 \cdot 10^6$.

Table 1. Thermodynamic atmospheric properties at 30 km altitude (U.S. Standard Atmosphere, 1976).

Altitude	Temperature	Pressure	Density	Mean free path	Sound speed	Dynamic viscosity
km	K	Pa	kg/m ³	m	m/s	N s /m ²
30	226.5	1197	0.01841	0.000004413	301.7	0.000014753

Table 2. Dimensionless quantities for Mach number 6.8 and 30 km.

Altitude	Knudsen number	Mach number	Velocity	Reynolds number
km	L=1 (m)		m/s	L=1 (m)
30	0.000004413	6.8	2051.59	$2.56 \cdot 10^6$

Note that the leading-edge angle of this present work, of generic scramjet inlet design, was assumed as 5.5° , the same leading-edge angle of the technological demonstrator scramjet 14-X B (Fig. 13) (Laitón et al, 2016). Considering a turbulent flow at the first ramp, which beginning at the leading edge, the maximum allowable turning angle without boundary-layer separation phenomena at the leading-edge angle of 5.5° is adequate.

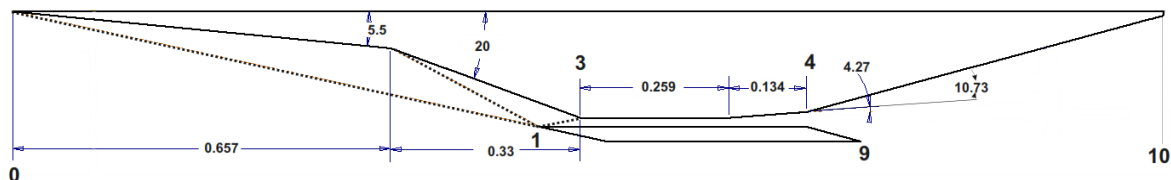


Figure 13. Cross section of the technological demonstrator 14-X B (Laitón et al., 2016).

Applying the scramjet inlet design by total pressure recovery and the maximum shockwave angles criterion, for a generic scramjet flying at a Mach number $M = 7$ through Earth's Atmosphere ($\gamma = 1.4$) at 30 km geometric altitude, it is found the following values of 5.92° , 6.98° and 8.22° . However, it is assumed the attached incident oblique shockwave angle at the leading-edge of 5.5° (to be consistent with the leading-edge of the scramjet 14-X B, Laitón et al., 2016), and the incident oblique shockwave angles establish at the corner of the compression ramps of 7° and 8.5° (Fig. 14).

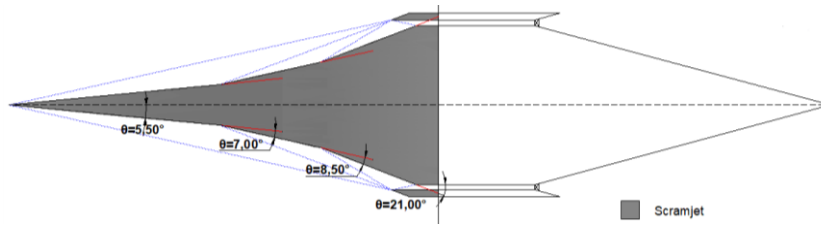


Figure 14. Cross section of the generic scramjet inlet.

The $\theta - \beta - M$ relation (Eq. 5) is applied to obtain the incident oblique shockwave angles as well as the reflected oblique shockwave angle (Tab. 3). Following, the thermodynamic air properties after each event (Tab. 3) may be evaluated by the thermodynamic property ratio (Eqs. 6-8) and the freestream thermodynamic properties (Tab. 1). The Mach number after each incident and reflected shockwave may be evaluated by Eq. 9 (Tab. 3).

The generic scramjet, with three ramps at the compression section (Fig. 14), with leading-edge angle of 5.5° , followed by two deflection angles of 7° and 8.5° , flying at 30 km of geometric altitude with speed corresponding at Mach number 6.8 is capable to generate a supersonic velocity corresponding to Mach number of 2.55 and a static temperature (Tab. 3) higher than 845.15 K, ignition temperature of hydrogen (Coordinating Research Council, 1983), at the entrance of combustion chamber. Consequently, it is possible to demonstrate a supersonic combustion when hydrogen may burn the supersonic atmospheric air, at the combustion chamber, during the atmospheric hypersonic flight of this generic scramjet.

Table 3. Thermodynamic properties at the generic scramjet engine inlet, non-viscous flow, calorically perfect gas ($p = \rho RT$, $\gamma = 1.4$).

		Freestream	Ramp 5.5°	Ramp 7°	Ramp 8.5°	Reflection
M_{in}		6.8	6.8	5.86	4.95	4.11
θ_{in}	$^\circ$		5.5°	7°	8.5°	21°
β_{out}	$^\circ$		12.47	15.04	18.12	33.22
M_{out}			5.86	4.95	4.11	2.55
$\frac{p_{out}}{p_{in}}$			2.35	2.54	2.60	5.76
$\frac{T_{out}}{T_{in}}$			1.30	1.34	1.35	1.90
$\frac{\rho_{out}}{\rho_{in}}$			1.81	1.90	1.93	3.02
p_{out}	Pa	1197	2813.18	7145.42	18582.81	106991.30
T_{out}	K	226.5	294.35	393.15	529.62	1008.64
ρ_{out}	kg/m^3	0.01841	0.03329	0.06331	0.12223	0.36952
a_{out}	m/s	301.7	343.94	397.49	461.35	636.67
u_{out}	m/s	2051.6	2018.08	1968.30	1897.37	1624.01
h_{total}	(J/kg)	2,332,014	2,332,052	2,332,102	2,332,113	2,332,089
T_{total}	K	2321.17	2321.14	2321.19	2321.20	2321.18
$M \text{ sen} \beta$	-		1.47	1.52	1.54	2.25
$\frac{p_{total e}}{p_{total i}}$	-		0.9393	0.9223	0.9166	0.6040

Note, the supersonic airflow across the plane attached shockwave promotes an increase of thermodynamic properties (pressure, temperature, density) and a decrease of flow velocity (Mach number), and the plane streamline of the airflow

remains supersonic and parallel to the flat surface (Tab. 3) of the generic scramjet starting at 5.5° leading-edge deflected angle.

It is calculated the values of the total enthalpy (Eq. 4) and the total temperature (Eq. 12) across each oblique incident and reflected shockwaves (Tab. 3). Note that the total enthalpy and the total temperature are conserved according to the energy conservation law.

$$T_{total} = \left(1 + \frac{\gamma - 1}{2} M^2\right) T \quad (12)$$

Also, the shockwave strength and the total pressure ratio are very close to each other due to the rounding of the deflection angles of the compression ramps (Tab. 3). Also, one may observe the total pressure ratio after the reflected shockwave decreased, compared to the total pressure ratio before the reflected shockwave due to the increase of the dissipation effects or the flow losses.

Table 4. Evaluation of momentum across each oblique incident and reflected shockwaves.

β	Before oblique shockwave	after oblique shockwave
5.5°	4812.06 (Pa)	4812.19 (Pa)
7.0°	11950.23 (Pa)	11950.28 (Pa)
8.5°	30873.66 (Pa)	30873.76 (Pa)
21°	150687.70 (Pa)	150688.53 (Pa)

Finally, the momentum (Eq. 2) across each oblique shockwave is (about) the same as the momentum conservation law predicted (Tab. 3). The value difference of the momentum across each oblique shockwave is due to the rounding of the deflection angles of the compression ramps.

4. CONCLUSION AND OUTLOOK FOR FUTURE PROJECTS

The principal aspects of design a scramjet obeying the fundamental conservation laws of physics are explored. Mass, momentum e energy conservation laws are applying to obtain not only the shock on-lip and shock on-corner conditions but also the maximization of the scramjet inlet (the turning, deflection, angles) by total pressure recovery and shockwave strength.

A generic scramjet has been designed, at the Universidade Federal do Rio Grande do Norte (UFRN), using analytical theoretical analysis (engineering approach), to fly at Earth's atmosphere at 30 km geometric altitude in Mach number 6.8 (2050 m/s), considering the atmospheric air behavior as a calorically perfect gas, from the tip-to-tail of the scramjet and the flow do not present viscous effects.

The 1D compressible flow, based on plane oblique shock wave, theory was applying to obtain the shockwave angle and the thermodynamic properties (pressure, temperature, density,...) and the flow velocity (Mach number) along the streamline of the non-viscous, calorically perfect air gas, flow.

The total pressure recovery and the strength of shockwave indicate, for a generic scramjet flying at a Mach number $M = 7$ through Earth's Atmosphere ($\gamma = 1.4$) at 30 km geometric altitude, the optimized turning angle were 5.92°, 6.98° and 8.22°. The turning (deflection) angles were rounding to 5.5° (to be consistent with the leading-edge of the scramjet 14-X B, a scramjet in developing at Instituto de Estudos Avançados/IEAv), and to 7° and 8.5°.

The generic scramjet, with three ramps at the compression section, with the turning angles of 5.5°, 7° and 8.5°, flying at 30 km of geometric altitude with speed corresponding at Mach number 6.8 is capable to generate a supersonic velocity corresponding to Mach number of 2.55 and a static temperature higher than 845.15 K, showing the possibility to burn hydrogen.

The supersonic/hypersonic atmospheric airflow across the oblique shockwave promotes an increase of thermodynamic properties and along the compression section of this generic scramjet inlet. The atmospheric supersonic air goes from the freestream 226.5 K to 1008 K in the combustion chamber, before mix and burn with hydrogen, showing the supersonic airflow must consider the high temperature effects. Also, this effort considers non-viscous effects in the supersonic airflow. Therefore, next steps not only the high temperature effects but also the viscous effects will be considering in the design of the generic scramjet.

5. ACKNOWLEDGEMENTS

The first five authors would like to thanks to Universidade Federal do Rio Grande do Norte (UFRN) the support given to complete this scientific work. The first author (as Visiting Professor) would like to express appreciation to UFRN the possibility to apply the knowledge in aerothermodynamics and hypersonics in the research area in hypersonic airbreathing propulsion based on supersonic combustion ramjet (scramjet) technology. This work has been

partially sponsored by European Space Research and Technology Centre (ESTEC) and the sixth author would like to extend his appreciation to support this project. Finally, a portion of this effort was supported by Instituto de Estudos Avançados (IEAv) and by the Propulsão Hipersônica 14-X (PropHiper) Project and the last author would like express his appreciation.

6. REFERENCES

- Anderson, J. D., Modern Compressible Flow, The Historical Perspective. McGraw-Hill, Inc., ed. 2nd, 1990.
- Coordinating Research Council, Inc. "Aviation Fuel Properties". CRC Report No. 530, September 1983.
- Hass, N.; Smart, M.; Paull, A. "Flight Data Analysis of the HYSHOT 2". AIAA/CIRA 13th International Space Planes and Hypersonics Systems and Technologies Conference. Capua, Italy. 2005.
- Heiser, W. H.; Pratt, D. T. *Hypersonic Airbreathing Propulsion*. Washington, D.C, American Institute of Aeronautics and Astronautics, 1994.
- Laitón, S. N. P.; Toro, P. G. P.; Rego, I. S.; Lima, B. C.; Martos, J. F. A. "Estudo teórico-analítico do veículo hipersônico aeroespacial Brasileiro". Congresso Nacional de engenharia Mecânica (CONEM). 2016.
- Martos, J. F. A. Aerothermodynamic design, manufacturing and testing of a 3-d prototyped scramjet. Thesis of Doctor in Science - Space Science and Technology, Space Propulsion and Hypersonics – Instituto Tecnológico de Aeronáutica, 2017.
- Moses, P. L.; Rausch, V. L; Nguyen, L. T.; Hill, J. R. "NASA hypersonic flight demonstrators – overview, status, and future plans". ACTA Astronautica, v. 55, p.619-630, 2004.
- Oswatitsch, K. "Pressure Recovery for Missiles with Reaction Propulsion at High Supersonic Speeds (The Efficiency of Shock Diffusers)". NACA Technical Memorandum 1140. 1947.
- Ran, H.; Mavris, D. Preliminary design of a 2D supersonic inlet to maximize total pressure recovery. AIAA5th Aviation, Technology, Integration, and Operations Conference. Arlington, Virginia, USA. 2005.
- Rolim, T. C., Minucci, M. A. S., Toro, P. G. P., and Soviero, P. A. O., 2009, "Experimental Results of a Mach 10 Conical-Flow Derived Waverider". 16th AIAA/DLR/DGLR International Space Planes and Hypersonic Systems and Technologies Conference. AIAA 2009-7433.
- U.S. Standard Atmosphere. NASA TM-X 74335. National Oceanic and Atmospheric Administration, National Aeronautics and Space Administration and United States Air Force. 1976.

7. RESPONSIBILITY NOTICE

The authors are the only responsible for the printed material included in this scientific article.

The authors declare that there is no conflict of interest regarding the publication of this scientific article.

Copyright ©2018 by P G. P. Toro. Published by the 17th Brazilian Congress of Thermal Sciences and Engineering (ENCIT 2018).